$$\mathrm{MR}(B) \equiv \frac{R(B) - R(0)}{R(0)} = \frac{I(0) - I(B)}{I(B)} \quad (3)$$

where $R(B)$ is the resistance at magnetic field B and $R(0)$ the resistance at zero field. We have derived $\mathrm{MR}_{max}(V)$ from the I-Vs for different channel lengths at zero magnetic field and maximum magnetic field, B_{max}, according to $\mathrm{MR}_{max}(V) = [I(V,0) - I(V,B_{max})]/I(V,B_{max})$, (Fig. 4C). The MR increases rapidly with decreasing voltage, reaching a maximum value of more than 2000% for 60-nm wire length when approaching 0 V. Because the current levels are below the noise limit close to 0 V, we have not been able to determine MR_{max} here.

The MR values in our molecular wires compare favorably with values reported for other systems under similar conditions. The highest room-temperature TMR value reported to date is 600% for an epitaxial CoFeB/MgO/CoFeB magnetic tunnel junction (*24*). Collosal magnetoresistance (CMR) manganites exhibit very large low-temperature MR at several tesla (*25*); however, room-temperature, low-field MR values are a few tens of percents (*26*, *27*). For nanocomposites containing magnetic nanoparticles, MR values similar to those in CMR experiments have been demonstrated under comparable experimental conditions (*28*). A large room-temperature MR effect of a few tens of percents was also reported for a graphene nanoribbon field-effect transistor (*29*).

We ascribe our very large MR values to the unique 1D character of our system. Indeed, nonstructured DXP thin films show much lower MR values (Fig. 4D). When a ~40-nm DXP film is contacted with a PtSi CP-AFM tip in the same setup, we measure a maximum MC of around –20%. With a Pt wire of 250-μm diameter instead of the PtSi tip, the maximum MC is reduced to about –5%. These results strongly suggest that confinement of the current path is crucial for explaining our results, in line with recent numerical studies (*9*). Explanations based on spin-dependent interactions involving excited states (*30*, *31*) can be ruled out, because the MR is also present—and even more pronounced—below the DXP HOMO-LUMO gap (~2 eV). The fact that for DXP the energy required to form doubly negatively charged states is remarkably small [~0.2 eV from cyclic voltammetry measurements (*23*)] suggests that such states are involved in transport. We therefore propose that the current is carried by electrons and that spin blockade is caused by two electrons residing on neighboring molecules attempting to form a doubly negatively charged molecule in a spin-singlet configuration by hopping of one of the electrons. The energetic disorder generally present in organic systems facilitates formation of doubly charged molecules at favorable locations. Moreover, the presence of a positively charged potassium ion close to a DXP molecule strongly reduces its LUMO level, also facilitating double charging. Simulations show that with these ingredients, MC values close to –100% indeed can be obtained with MC (B) curves having the line shape of Eq. 2 (*10*). Further analysis should provide more insight into the details of the mechanism behind the effect, but the present experimental results clearly point at spin blockade tuned by a competition between the external magnetic field and the random internal hyperfine field.

References and Notes

1. M. N. Baibich *et al.*, *Phys. Rev. Lett.* **61**, 2472–2475 (1988).
2. G. Binasch, P. Grünberg, F. Saurenbach, W. Zinn, *Phys. Rev. B* **39**, 4828–4830 (1989).
3. M. Jullière, *Phys. Lett.* **54**, 225–226 (1975).
4. J. S. Moodera, L. R. Kinder, T. M. Wong, R. Meservey, *Phys. Rev. Lett.* **74**, 3273–3276 (1995).
5. K. Ono, D. G. Austing, Y. Tokura, S. Tarucha, *Science* **297**, 1313–1317 (2002).
6. R. Hanson, L. P. Kouwenhoven, J. R. Petta, S. Tarucha, L. M. K. Vandersypen, *Rev. Mod. Phys.* **79**, 1455–1455 (2007).
7. T. Francis, Ö. Mermer, G. Veeraraghavan, M. Wohlgenannt, *New J. Phys.* **6**, 185 (2004).
8. W. Wagemans *et al.*, *Spin* **1**, 93–108 (2011).
9. S. P. Kersten, S. Meskers, P. A. Bobbert, *Phys. Rev. B* **86**, 045210 (2012).
10. Materials and methods are available as supplementary materials on *Science* Online.
11. G. Calzaferri, S. Huber, H. Maas, C. Minkowski, *Angew. Chem. Int. Ed.* **42**, 3732–3758 (2003).
12. P. Bornhauser, G. Calzaferri, *J. Phys. Chem.* **100**, 2035–2044 (1996).
13. P. A. Anderson *et al.*, *Dalton Trans.* **19**, 3122–3128 (2004) and references therein.
14. M. J. Kelly, *J. Phys. Condens. Matter* **7**, 5507–5519 (1995).
15. T. Bein, in *Recent Advances and New Horizons in Zeolite Science and Technology*, H. Chon, S. I. Woo, S. E. Park, Eds. (Elsevier, Amsterdam, 1996), pp. 295–322.
16. D. J. Cardin, *Adv. Mater.* **14**, 553 (2002).
17. U. Simon, M. E. Franke, in *Host-Guest-Systems Based on Nanoporous Crystals*, F. Laeri, F. Schüth, U. Simon, M. Wark, Eds. (Wiley, Weinheim, 2003), pp. 364–378.
18. M. Álvaro *et al.*, *Chem. Mater.* **18**, 26–33 (2006).
19. F. J. Jansen, R. A. Schoonheydt, *J. Chem. Soc., Faraday Trans.* **69**, 1338 (1973).
20. Z. K. Tang *et al.*, *Science* **292**, 2462 (2001).
21. A. M. Nardes *et al.*, *Org. Electron.* **9**, 727–734 (2008).
22. H. Bentmann, A. A. Demkov, R. Gregory, S. Zollner, *Phys. Rev. B* **78**, 205302 (2008).
23. S. K. Lee *et al.*, *J. Am. Chem. Soc.* **121**, 3513–3520 (1999).
24. S. Ikeda *et al.*, *Appl. Phys. Lett.* **93**, 082508 (2008).
25. G. Q. Gong *et al.*, *Appl. Phys. Lett.* **67**, 1783 (1995).
26. P. K. Siwach, H. K. Singh, O. N. Srivastava, *J. Phys. Condens. Matter* **20**, 273201 (2008).
27. Y.-T. Zhang, Z.-Y. Chen, C.-C. Wang, Q. Jie, H.-B. Lü, *J. Magn. Magn. Mater.* **321**, 1199–1201 (2009).
28. F. J. Yue *et al.*, *J. Phys. D Appl. Phys.* **44**, 025001 (2011).
29. J. Bai *et al.*, *Nat. Nanotechnol.* **5**, 655–659 (2010).
30. V. N. Prigodin, J. D. Bergeson, D. M. Lincoln, A. J. Epstein, *Synth. Met.* **156**, 757–761 (2006).
31. P. Desai, P. Shakya, T. Kreouzis, W. P. Gillin, *Phys. Rev. B* **76**, 235202 (2007).

Acknowledgments: We thank B. Koopmans, L. Abelmann, L. P. Kouwenhoven, Y. Tokura, and S. Tarucha for fruitful discussions. We acknowledge financial support from the Netherlands Technology Foundation STW, the European Research Council, ERC Starting Grant nos. 240433 and 280020, ERC Advanced Grant no. 247365, NanoScience Europe program (NanoSci-ERA), grant no. 11003, and the Foundation for Fundamental Research on Matter (FOM), part of the Netherlands Organisation for Scientific Research (NWO). A link to the data reported here is included in the supplementary materials. R.N.M. and M.H.S. carried out the magnetoresistance experiments and performed the data analysis. H.L. performed the zeolite L crystal synthesis and molecular loading. W.G.v.d.W. conceived the experiments and planned and supervised the project. L.D.C. conceived the project together with W.G.v.d.W. and supervised the zeolite synthesis and loading. S.P.K. and P.A.B. performed the theoretical analysis and numerical simulations. M.P.d.J. contributed to planning and supervision. All authors discussed the results, provided important insights, and helped write the manuscript.

Supplementary Materials

www.sciencemag.org/cgi/content/full/science.1237242/DC1
Materials and Methods
Figs. S1 to S4
Data Files
References (*32*–*37*)

1 March 2013; accepted 14 June 2013
Published online 4 July 2013;
10.1126/science.1237242

Isotope Ratios of H, C, and O in CO_2 and H_2O of the Martian Atmosphere

Chris R. Webster,[1]* Paul R. Mahaffy,[2] Gregory J. Flesch,[1] Paul B. Niles,[6] John H. Jones,[7] Laurie A. Leshin,[3] Sushil K. Atreya,[4] Jennifer C. Stern,[2] Lance E. Christensen,[1] Tobias Owen,[5] Heather Franz,[2] Robert O. Pepin,[8] Andrew Steele,[9] the MSL Science Team†

Stable isotope ratios of H, C, and O are powerful indicators of a wide variety of planetary geophysical processes, and for Mars they reveal the record of loss of its atmosphere and subsequent interactions with its surface such as carbonate formation. We report in situ measurements of the isotopic ratios of D/H and $^{18}O/^{16}O$ in water and $^{13}C/^{12}C$, $^{18}O/^{16}O$, $^{17}O/^{16}O$, and $^{13}C^{18}O/^{12}C^{16}O$ in carbon dioxide, made in the martian atmosphere at Gale Crater from the Curiosity rover using the Sample Analysis at Mars (SAM)'s tunable laser spectrometer (TLS). Comparison between our measurements in the modern atmosphere and those of martian meteorites such as ALH 84001 implies that the martian reservoirs of CO_2 and H_2O were largely established ~4 billion years ago, but that atmospheric loss or surface interaction may be still ongoing.

The Sample Analysis at Mars (SAM) suite (*1*) on the Curiosity rover that landed in August 2012 is conducting a search for organic compounds and volatiles in rocks and soils and characterizing the chemical and isotopic composition of the modern atmosphere. Atmo-

spheric characterization is one of the exploration goals of the Mars Science Laboratory (MSL) mission (*2*), and it is accomplished using SAM's tunable laser spectrometer (TLS) and its quadrupole mass spectrometer (QMS). Here we focus on TLS measurements; a companion paper (*3*) focuses on those from the QMS. Results for nondetection by TLS of atmospheric methane are reported elsewhere (*4*).

Previous measurements of isotopes of H, N, and noble gases in the martian atmosphere to date (*5*) have indicated enrichment in the heavier isotopes, consistent with the idea of atmospheric loss to space of the lighter isotopes (*6*, *7*). Although meteoritic analyses of $\delta^{13}C$ and $\delta^{18}O$ (*8*) in shergottite, nakhlite, and chassigny (SNC)–class meteorites are made at higher precision than the atmospheric measurements to date, they are challenged to correctly account for possible terrestrial contamination (*9*). Measurements of CO_2 isotopes at Mars and in particular $\delta^{13}C$ values have not been consistent with atmospheric loss (*10*). Viking (*11*) measured $\delta^{13}C$ and $\delta^{18}O$ values of 23 ± 43 per mil (‰) and 7 ± 44‰. Earth-based spectroscopy has suggested depleted values for $\delta^{13}C$ of –22 ± 20‰ and $\delta^{18}O$ of 18 ± 18‰ (*9*). The recent Phoenix lander measured $\delta^{13}C$ and $\delta^{18}O$ values for CO_2 in the martian atmosphere of –2.5 ± 4.3‰ and 31 ± 5.7‰, respectively (*12*). Although uncertainties in these earlier atmospheric measurements of $\delta^{13}C$ and $\delta^{18}O$ overlap (Table 1), their $\delta^{13}C$ values are in marked contrast to measurements of trapped CO_2 in martian meteorite EETA 79001, generally considered to be closest to the true martian atmosphere and which yielded a $\delta^{13}C$ of 36 ± 10‰ (*8*).

For D/H in water, the difference in ground-state energies of HDO and its parent HHO are large enough to cause large changes in δD in equilibrium and nonequilibrium (kinetic) processes (*13*, *14*), especially where condensation or freezing occurs. For this reason, D/H has become a universally important ratio to identify planetary origin and history (*7*, *15*). The 1988 telescopic observation of D/H values in the martian atmosphere that were ~6 times that of Earth (*7*) were pivotal in the idea of atmospheric loss to space from a dense, warm, ancient atmosphere. Initial measurements in meteorites (*16*) gave a wide range of D/H values that may have included terrestrial contributions. A more recent analysis (*17*) of the ancient meteorite ALH84001 (~4 billion years old) and young meteorite Shergotty (0.17 billion years old) produced δD values of 3000 and 4600, respectively. These results have been interpreted (*17*) as evidence for a two-stage evolution for Martian water—a significant early loss of water to space [before 3.9 billion years ago (Ga)], followed by only modest loss to space during the past 4 billion years. Until Curiosity landed, there had been no in situ measurements of the water isotopic species HDO and $H_2{}^{18}O$.

Oxygen isotopes in carbonates and sulfates from martian meteorites do not show any enrichment in $\delta^{18}O$ and therefore have not been used as indicators of atmospheric escape (*18*, *19*). It has been suggested that they are buffered by interaction with a larger O reservoir such as the silicates in the crust, or crustal ice deposits (*20*), although this is complicated by evidence for disequilibrium between the crust and the atmosphere (*21*). Oxygen isotopes in CO_2 and H_2O are therefore likely indicators of more complex interactions between the large reservoir of O in the hydrosphere, lithosphere, and atmosphere of Mars.

TLS is a two-channel tunable laser spectrometer that uses direct and second harmonic detection of infrared (IR) laser light absorbed after

Table 1. Carbon dioxide isotope ratios ‰ ± 2 SEM (standard error of the mean). *, not measured.

Measurement	$\delta^{13}C$	$\delta^{18}O$	$\delta^{17}O$	$\delta^{13}C^{18}O$
SAM-TLS	46 ± 4	48 ± 5	24 ± 5	109 ± 31
SAM-QMS (*3*)	45 ± 12	*	*	*
Phoenix lander (*12*)	–2.5 ± 4.3	31.0 ± 5.7	*	*
Viking Neutral Mass Spectrometer (*11*)	23 ± 43	7 ± 44	*	*
SNC meteorites (*8*, *12*, *32*)	36 ± 10	3.9–5.4 ± 0.1	~0.53* $\delta^{18}O$ ~ $\delta^{13}C$+ $\delta^{18}O$	
ALH84001 meteoritic carbonate range (*30*, *31*)	27 to 64	–9 to 26	~0.53* $\delta^{18}O$ ~ $\delta^{13}C$+ $\delta^{18}O$	
ALH84001 meteoritic carbonate mean value (*31*)	46 ± 8	4.6 ± 1.2	*	*
Earth telescopes (*9*)	–22 ± 21	18 ± 18	*	*

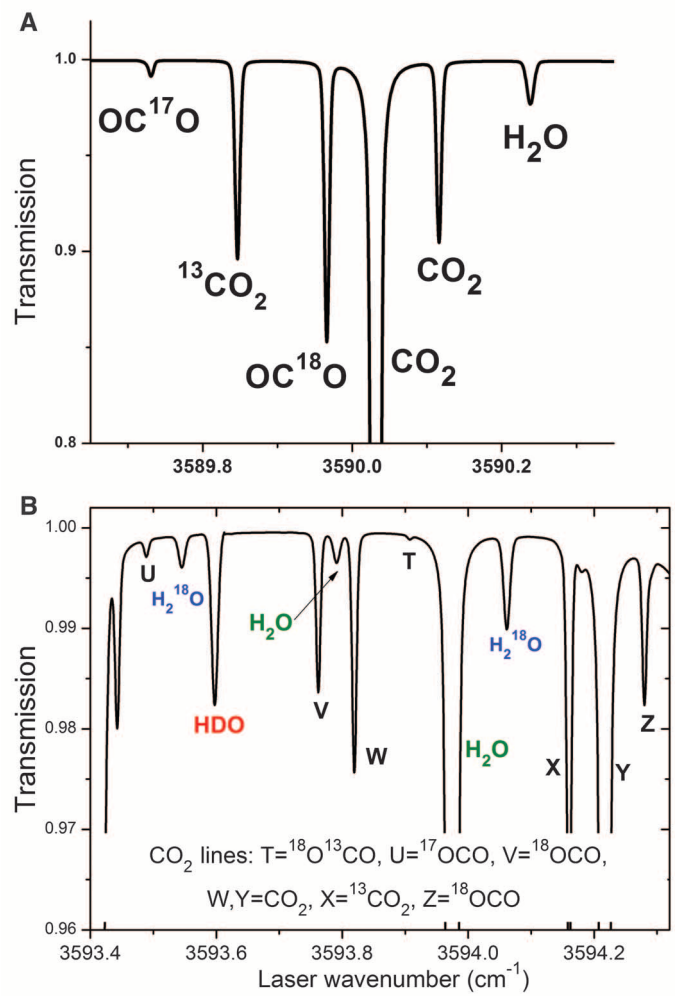

Fig. 1. Spectral scan regions used by the TLS instrument. Calculated spectra from the HITRAN database (*36*) for measuring CO_2 (**A** and **B**) and H_2O isotope ratios (B). The HDO line intensity has been increased by a factor of 6 to better represent the martian environment.

[1]Jet Propulsion Laboratory, California Institute of Technology, Pasadena, CA 91109, USA. [2]NASA Goddard Space Flight Center, Greenbelt, MD 20771, USA. [3]Rensselaer Polytechnic Institute, Troy, NY 12180, USA. [4]University of Michigan, Ann Arbor, MI 48105, USA. [5]University of Hawaii, Honolulu, HI 96822, USA. [6]NASA Johnson Space Center, Houston, TX 77058, USA. [7]University of Arizona, Tucson, AZ 85721, USA. [8]University of Minnesota, Minneapolis, MN 55455, USA. [9]Carnegie Institution of Washington, Washington, DC 20015, USA.

*Corresponding author. E-mail: chris.r.webster@jpl.nasa.gov
†Mars Science Laboratory (MSL) Science Team authors and affiliations are listed in the supplementary materials.

multipassing a sample cell (*1*). One laser source is a near-IR tunable diode laser at 2.78 μm that can scan two spectral regions containing CO_2 and H_2O isotopic lines; the second laser source is an interband cascade laser at 3.27 μm used for methane detection alone (*4*). The near-IR laser makes 43 passes of a 20-cm-long sample (Herriott) cell that is evacuated with a turbomolecular pump for background scans, then filled to 0.7 mbar using volume expansion of Mars air originally at ~7 mbar. TLS scans over individual rovibrational lines in two spectral regions near 2.78 μm; one centered at 3590 cm^{-1} for CO_2 isotopes and a second centered at 3594 cm^{-1} for both CO_2 and H_2O isotopes (Figs. 1 and 2). The lines used in both regions have no significant interferences. In the 3594 cm^{-1} region, the CO_2 and H_2O lines we used interleave across the spectrum without interference, allowing the determination of accurate isotope ratios across widely varying CO_2 and H_2O abundances in both atmospheric and evolved gas experiments. The laser scans every second through the target spectral regions. Each 1-s spectrum is then co-added on board in 2-min periods, and the averaged spectra are then downlinked as raw data during a given run, typically of ~30 min duration. Data reported here were collected from 6 days (martian sols 28, 53, 73, 79, 81, and 106). During data collection, the Herriott cell and other optics are kept at 47° ± 3°C using a ramped heater that also serves to increase the signal-to-noise ratio in spectra by reducing the effect of interference fringes occurring during the 2-min sample period. The measured background amounts (empty cell) of both CO_2 and H_2O are negligible and also reflect an insignificant contribution to the signal from the instrument foreoptics. TLS is calibrated using certified isotopic standards (*22*) that improve the accuracy of isotope ratios over using the more uncertain HITRAN (high-resolution transmission molecular absorption) database spectral parameters.

Our CO_2 isotope ratios (Table 1, table S1, and Fig. 3) are given relative to Vienna Pee Dee belmnite (VPDB) for $\delta^{13}C$ and relative to Vienna standard mean ocean water (VSMOW) for all oxygen isotopes (*13*). The measured value of $\delta^{13}C^{18}O$ agrees within uncertainty to the sum of the individual $\delta^{13}C$ and $\delta^{18}O$ measurements, providing a valuable check-sum on our results. Also, our measured value for $\delta^{17}O$ is half that of $\delta^{18}O$, as predicted from mass-dependent fractionation ($\delta^{17}O = 0.528 \times \delta^{18}O$) and consistent with previous SNC meteorite analysis. The independent SAM QMS result for $\delta^{13}C$ of 45 ± 12‰ (*3*) agrees well with that from TLS at 46 ± 4‰, both values notably disagreeing with the much lower Phoenix lander result (*12*) of –2.5 ± 4.3‰. The sol-by-sol data plotted in Fig. 3 is not over a sufficiently long period to assess possible seasonal variation in $\delta^{13}C$ or $\delta^{18}O$.

Our measured water abundances of up to 1% by volume in our Herriott cell after atmospheric intake exceed those expected (~150 parts per million by volume) in martian air, and allowed us to retrieve a value for atmospheric δD, although with high uncertainty. Because our measured highly enriched δD values (Table 2 and table S2) are clearly martian and not terrestrial, we attribute the high water mixing ratios to either high near-surface humidity (natural or from enhanced temperatures in the vicinity of the rover) or to water entrained from frozen or liquid sources on or near the heated inlet valve. Also, in evolved gas experiments from pyrolysis of Rocknest fines (*23*), water was seen coming off at relatively low temperatures that we here identify as representative of the δD and $\delta^{18}O$ values of the martian atmosphere. The TLS measurement of δD agrees well with observations from ground-based telescopes (*24*), but the contribution from expected seasonal cycling (*25*) is unknown. The enriched atmospheric values contrast with the low primordial D/H values postulated for the martian mantle (*26*) and are higher than those from our Rocknest higher-temperature studies (*23*).

Modeling estimates of escape processes and atmospheric stability during Mars' initial history point to catastrophic loss of atmospheric mass, and suggest that many atmospheric species carrying records of early isotopic evolution did not survive beyond approximately 3.7 to 4 Ga (*27*, *28*). Carbonates in the ALH 84001 meteorite derived from an alteration event that occurred at ~3.9 Ga (*29*) preserve our best record of these events. Measurements of ALH 84001 carbonates show enriched isotopic values of $\delta^{13}C$ = +27 to +64‰ (*30*, *31*), δD values of ~3000‰ (*16*, *17*), and low

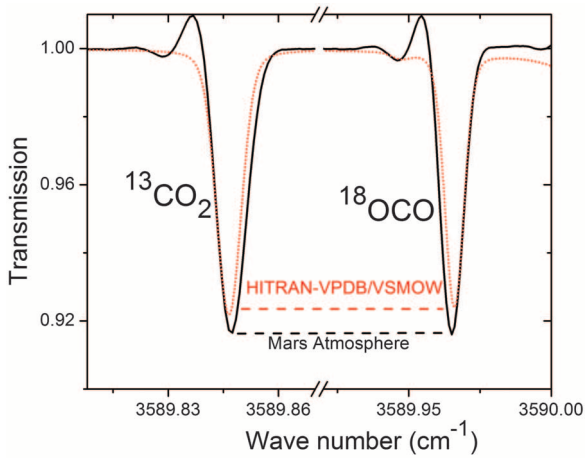

Fig. 2. Observed versus calculated spectra. A single spectrum (middle section) downloaded from Curiosity (black), showing observed enrichment in $^{13}CO_2$ and ^{18}OCO compared to the calculated HITRAN spectrum (red) based on terrestrial (VPDB and VSMOW) isotope ratios (*36*). Both spectra are normalized in depth to the $^{16}O^{12}C^{16}O$ line near 3590.1 cm^{-1} (Fig. 1). Ringing to the left side of the lines is explained in (*22*).

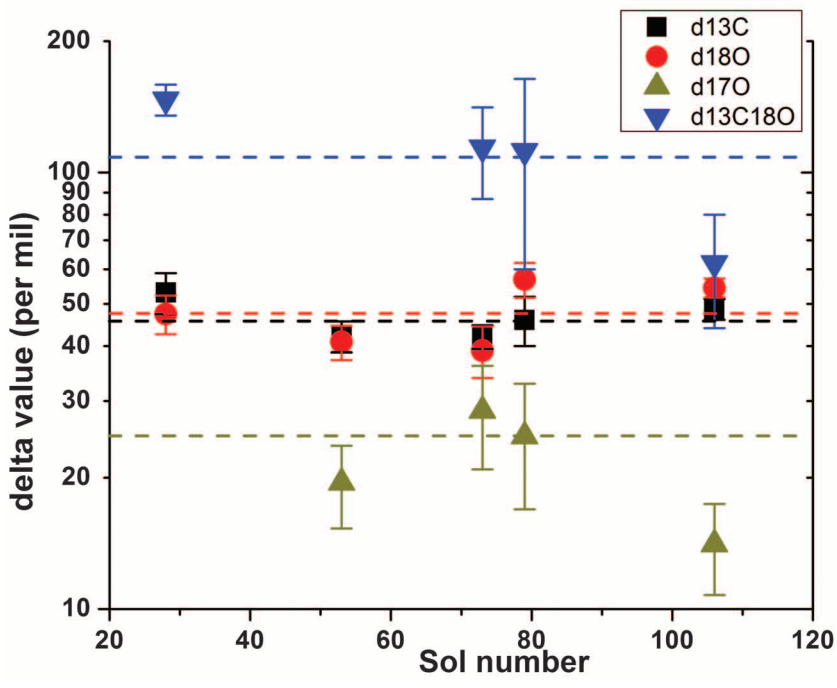

Fig. 3. Sol-by-sol mean values for CO_2 isotope ratios. The mean values for all sols combined (dashed lines) are given in Table 1. See (*22*) for values and uncertainties of the individual sol data plotted.

Table 2. Water isotope ratios ‰ ± 2 SEM. *, not measured.

Measurement	δD	$\delta^{18}O$
SAM-TLS atmosphere	4950 ± 1,080	*
SAM-TLS evolved water: Rocknest fines 230° to 430°C (*23*)	5880 ± 60	84 ± 10
Meteoritic crustal reservoirs (*26*)	~5000	*
Earth telescopes (*24*)	1700–8900	*
ALH 84001 (*17*)	3000	*
Shergotty USNM 321-1 (*17*)	4600	*

$\delta^{18}O$ values (*32*). These values are similar to the composition of the modern martian atmosphere, suggesting that the $\delta^{13}C$, δD, and $\delta^{18}O$ of the martian atmosphere were enriched early and have not changed much over ~4 billion years. Our higher values of δD and $\delta^{18}O$ measured in the atmosphere suggest that escape processes may have also continued since 4.0 Ga, in accordance with a two-stage evolutionary process (*17*) described above.

We observe large enrichments of $\delta^{18}O$ in atmospheric water vapor and CO_2. The $\delta^{18}O$ values of the water vapor are much larger than the $\delta^{18}O$ observed in carbonates and sulfates in martian meteorites and suggest that the oxygen in water vapor in the martian atmosphere is not in equilibrium with the crust (*33*, *34*) and could have been enriched in heavy isotopes through atmospheric loss. Another possibility is that the elevated oxygen isotope values in the more abundant martian CO_2 are being transferred to the water vapor through photochemical reactions in the atmosphere. However, $\delta^{18}O$ values of CO_2 in Earth's atmosphere are similarly elevated because of low-temperature equilibration between CO_2 and H_2O, and this process could also be operative on Mars (*12*).

In addition to atmospheric loss, other processes such as volcanic degassing and weathering might act to change the isotopic composition of the atmosphere through time. Estimates for the magnitude of these two contributions over the ~4-billion-year history of Mars vary widely (*30*, *34*, *35*), yet could have a strong impact on the isotopic composition of the atmosphere and challenge the status quo model described above.

References and Notes

1. P. R. Mahaffy *et al.*, *Space Sci. Rev.* **170**, 401–478 (2012).
2. J. P. Grotzinger *et al.*, *Space Sci. Rev.* **170**, 5–56 (2012).
3. P. R. Mahaffy *et al.*, *Science* **341**, 263–266 (2013).
4. C. R. Webster, P. R. Mahaffy, S. K. Atreya, G. J. Flesch, K. A. Farley, *Lunar Planet. Sci. Conf.*, abstract 1366 (2013).
5. B. M. Jakosky, R. J. Phillips, *Nature* **412**, 237–244 (2001).
6. M. B. McElroy, Y. L. Yung, A. O. Nier, *Science* **194**, 70–72 (1976).
7. T. Owen, J.-P. Maillard, C. de Bergh, B. L. Lutz, *Science* **240**, 1767–1770 (1988).
8. R. H. Carr, M. M. Grady, I. P. Wright, C. T. Pillinger, *Nature* **314**, 248–250 (1985).
9. V. A. Krasnopolsky, J. P. Maillard, T. C. Owen, R. A. Toth, M. D. Smith, *Icarus* **192**, 396–403 (2007).
10. P. B. Niles *et al.*, *Space Sci. Rev.* **174**, 301–328 (2013).
11. A. O. Nier, M. B. McElroy, *Science* **194**, 1298–1300 (1976).
12. P. B. Niles, W. V. Boynton, J. H. Hoffman, D. W. Ming, D. Hamara, *Science* **329**, 1334–1337 (2010).
13. R. E. Criss, *Principles of Stable Isotope Composition* (Oxford Univ. Press, Oxford, 1999).
14. C. R. Webster, A. J. Heymsfield, *Science* **302**, 1742–1745 (2003).
15. P. Hartogh *et al.*, *Nature* **478**, 218–220 (2011).
16. L. A. Leshin, S. Epstein, E. M. Stolper, *Geochim. Cosmochim. Acta* **60**, 2635–2650 (1996).
17. J. P. Greenwood, S. Itoh, N. Sakamoto, E. P. Vicenzi, H. Yurimoto, *Geophys. Res. Lett.* **35**, L05203 (2008).
18. J. Farquar, M. H. Thiemens, *J. Geophys. Res.* **105**, (2000).
19. C. S. Romanek *et al.*, *Nature* **372**, 655–657 (1994).
20. B. Jakosky, A. Zent, R. Zurek, *Icarus* **130**, 87–95 (1997).
21. H. R. Karlsson, R. N. Clayton, E. K. Gibson Jr., T. K. Mayeda, *Science* **255**, 1409–1411 (1992).
22. See the supplementary materials on *Science* Online.
23. L. A. Leshin *et al.*, *Lunar Planet. Sci. Conf.*, abstract 2220 (2013).
24. D. A. Fisher, *Icarus* **187**, 430–441 (2007) and references therein.
25. R. E. Novak *et al.*, *Bull. Am. Astron. Soc.* **35**, 660 (2005).
26. T. Usui, C. Alexander, J. Wang, J. Simon, J. Jones, *Earth Planet. Sci. Lett.* **357-358**, 119–129 (2012).
27. H. Lammer *et al.*, *Space Sci. Rev.* **174**, 113–154 (2013).
28. R. O. Pepin, *Icarus* **111**, 289–304 (1994).
29. L. Borg, M. J. Drake, *J. Geophys. Res.* **110**, E12S03 (2005).
30. P. B. Niles, L. A. Leshin, Y. Guan, *Geochim. Cosmochim. Acta* **69**, 2931–2944 (2005).
31. J. W. Valley *et al.*, *Science* **275**, 1633–1638 (1997).
32. J. Farquhar, D. T. Johnston, *Rev. Mineral. Geochem.* **68**, 463–492 (2008).
33. B. M. Jakosky, J. H. Jones, *Nature* **370**, 328–329 (1994).
34. M. Grott, A. Morschhauser, D. Breuer, E. Hauber, *EPSL* **308**, 391–400 (2011).
35. J. P. Bibring *et al.*, *Science* **312**, 400–404 (2006).
36. L. S. Rothman *et al.*, *J. Quant. Spectrosc. Radiat. Transf.* **110**, 533–572 (2009).

Acknowledgments: The research described here was carried out at the Jet Propulsion Laboratory, California Institute of Technology, under a contract with NASA.

Supplementary Materials

www.sciencemag.org/cgi/content/full/341/6143/260/DC1
Materials and Methods
Supplementary Text
Figs. S1 to S3
Tables S1 to S4
Reference (*37*)
MSL Science Team Authors and Affiliations

18 March 2013; accepted 17 June 2013
10.1126/science.1237961

Abundance and Isotopic Composition of Gases in the Martian Atmosphere from the Curiosity Rover

Paul R. Mahaffy,[1]* Christopher R. Webster,[2] Sushil K. Atreya,[3] Heather Franz,[1] Michael Wong,[3] Pamela G. Conrad,[1] Dan Harpold,[1] John J. Jones,[4] Laurie A. Leshin,[5] Heidi Manning,[6] Tobias Owen,[7] Robert O. Pepin,[8] Steven Squyres,[9] Melissa Trainer,[1] MSL Science Team†

Volume mixing and isotope ratios secured with repeated atmospheric measurements taken with the Sample Analysis at Mars instrument suite on the Curiosity rover are: carbon dioxide (CO_2), 0.960(±0.007); argon-40 (^{40}Ar), 0.0193(±0.0001); nitrogen (N_2), 0.0189(±0.0003); oxygen, 1.45(±0.09) × 10^{-3}; carbon monoxide, < 1.0 × 10^{-3}; and $^{40}Ar/^{36}Ar$, 1.9(±0.3) × 10^3. The $^{40}Ar/N_2$ ratio is 1.7 times greater and the $^{40}Ar/^{36}Ar$ ratio 1.6 times lower than values reported by the Viking Lander mass spectrometer in 1976, whereas other values are generally consistent with Viking and remote sensing observations. The $^{40}Ar/^{36}Ar$ ratio is consistent with martian meteoritic values, which provides additional strong support for a martian origin of these rocks. The isotopic signature $\delta^{13}C$ from CO_2 of ~45 per mil is independently measured with two instruments. This heavy isotope enrichment in carbon supports the hypothesis of substantial atmospheric loss.

The science and exploration goal of the Mars Science Laboratory (MSL) (*1*) is to advance our understanding of the potential of the present or past martian environments to support life. An understanding of how the present environment in Gale crater differs from the environment at the time of its formation requires comprehensive chemical characterization. The first set of experiments of the Sample Analysis at Mars (SAM) investigation (*2*) (Fig. 1) of the Curiosity rover included measurements of the chemical and isotopic composition of the atmosphere with sequences that employed two of SAM's three instruments. When

Science

Isotope Ratios of H, C, and O in CO_2 and H_2O of the Martian Atmosphere

Chris R. Webster, Paul R. Mahaffy, Gregory J. Flesch, Paul B. Niles, John H. Jones, Laurie A. Leshin, Sushil K. Atreya, Jennifer C. Stern, Lance E. Christensen, Tobias Owen, Heather Franz, Robert O. Pepin, Andrew Steele and the MSL Science Team

Science **341** (6143), 260-263.
DOI: 10.1126/science.1237961

Mars' Atmosphere from Curiosity

The Sample Analysis at Mars (SAM) instrument on the Curiosity rover that landed on Mars in August last year is designed to study the chemical and isotopic composition of the martian atmosphere. **Mahaffy *et al.*** (p. 263) present volume-mixing ratios of Mars' five major atmospheric constituents (CO_2, Ar, N_2, O_2, and CO) and isotope measurements of $^{40}Ar/^{36}Ar$ and C and O in CO_2, based on data from one of SAM's instruments, obtained between 31 August and 21 November 2012. **Webster *et al.*** (p. 260) used data from another of SAM's instruments obtained around the same period to determine isotope ratios of H, C, and O in atmospheric CO_2 and H_2O. Agreement between the isotopic ratios measured by SAM with those of martian meteorites, measured in laboratories on Earth, confirms the origin of these meteorites and implies that the current atmospheric reservoirs of CO_2 and H_2O were largely established after the period of early atmospheric loss some 4 billion years ago.